
Structured Q-learning For Antibody Design

Alexander I. Cowen-Rivers
Technische Universität Darmstadt

Philip John Gorinski
Huawei R&D

Aivar Sootla
Huawei R&D

Asif Khan
University of Edinburgh

Furui Liu
Huawei R&D

Jun Wang
Huawei R&D
University College London

Jan Peters
Technische Universität Darmstadt

Haitham Bou Ammar
Huawei R&D
University College London

Abstract

Optimizing combinatorial structures is core to many real-world problems, such as those encountered in life sciences. For example, one of the crucial steps involved in antibody design is to find an arrangement of amino acids in a protein sequence that improves its binding with a pathogen. Combinatorial optimization of antibodies is difficult due to extremely large search spaces and non-linear objectives. Even for modest antibody design problems, where proteins have a sequence length of eleven, we are faced with searching over 2.05×10^{14} structures. Applying traditional Reinforcement Learning algorithms such as Q-learning to combinatorial optimization results in poor performance. We propose Structured Q-learning (SQL), an extension of Q-learning that incorporates structural priors for combinatorial optimization. Using a molecular docking simulator, we demonstrate that SQL finds high binding energy sequences and performs favourably against baselines on eight challenging antibody design tasks, including designing antibodies for SARS-COV.

1 Introduction

Combinatorial optimization is a general problem faced in many domains, wherein one is tasked with finding an ordered or unordered placement of combinatorial variables with the goal of maximising an objective function. Combinatorial problems with known objectives include maximum satisfiability (*MaxSAT*) applications such as program synthesis [1], program verification [2] and automated theorem proving [3–5]. In engineering, combinatorial problems include finding optimal chip configurations[6], compiler optimization[7] and logic synthesis[8]. In logistics, combinatorial problems include travelling salesman problems [9–11] and solving extremely large linear systems with constraints, commonly referred to as mixed-integer linear programming [12–17]. Lastly, in life sciences combinatorial problems involve core structures such as DNA, mRNA, and proteins, as well as functional molecules represented by SMILES [18] or SELFIES [19] strings. These fundamental combinatorial structures are central to medical breakthroughs such as the development of proteins to target cancer tumours [20], as well developing mRNA vaccines for SARS-COV2 [21].

On the complexity of combinatorial optimization: Combinatorial optimization is extremely challenging. Taking *MaxSAT* problems as an example, a well-studied family of combinatorial optimization problems within computational complexity theory, they only deal with Boole variables (with cardinality $n = 2$), yet are proven to be NP-hard [22, 23]. Maximum satisfiability modulo theories (*MaxSMT*) [24] extends *MaxSAT* to handle complex combinatorial variables such as; bit vectors,

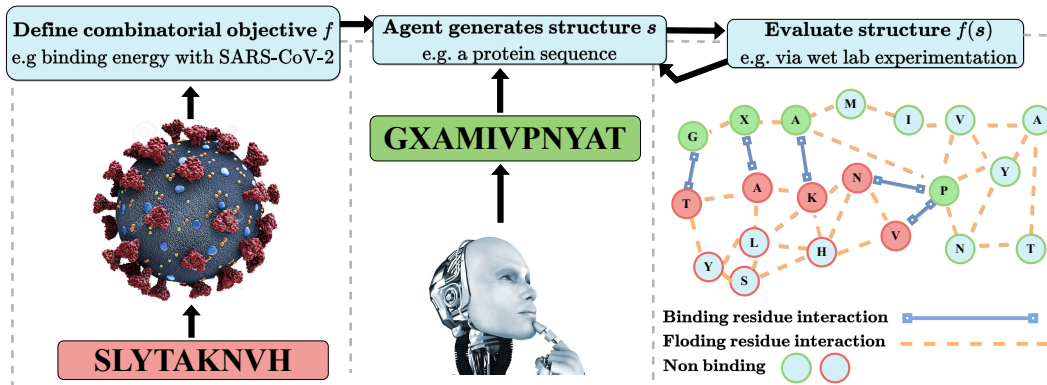


Figure 1: Illustrative example showing combinatorial optimization of an antibody using RL.

strings, ordinal and categorical with higher cardinality ($n \gg 2$). *MaxSMT* better resembles the optimization problems found within life sciences, as structures like DNA, proteins and SELFIES have corresponding cardinality $n = 4, n = 20, n \approx 500$. *MaxSMT* solvers rely on quantifier elimination algorithms [25–28] such as Cylindrical Algebraic Decomposition [29] (CAD). However, CAD’s worst case complexity is **doubly exponential** in the number of variables [29–31] i.e. $\mathcal{O}(2^{2^{L+1}})$, highlighting the undesirable difficulty faced in combinatorial optimization *even when the objective function is known*.

Motivation: When there is nothing known about the objective function, one can only *learn* about the inter-relationships between variables and their evaluation. Deep Reinforcement Learning (RL) has seen great success in many challenging applications, such as generating solutions to the NP-hard [32] Travelling Salesman Problem [33, 10] (TSP), GO [34] as well as controlling plasma [35]. Structural priors have been proposed for policy gradients [33, 10] which improve combinatorial optimization, yet we have not seen structural priors developed for off-policy algorithms such as Q-learning.

The contributions of this work are three-fold: (i) We introduce *Structured Q-learning (SQL)*, an extension of Q-learning equipped with structural priors such as structure critic targets, structure policy evaluation, structure exploration operator and structure policy improvement. (ii) Using a molecular docking simulator, we show the structural priors introduced allow SQL improves upon its unstructured and on-policy counterparts on a challenging suite of antibody design tasks.

2 Related Work

The Machine Learning for Combinatorial optimization (ML4CO) [36] competition ¹ was recently, hosted where competitors provide ML algorithms to improve the efficiency of solving Mixed Integer Programming (MIP) and Mixed Integer Nonlinear Programming (MINLP) problems, compared to SOTA solvers such as SCIP [12]. The combinatorial optimization approaches can be classified into two broad categories: those that fully rely on ML models to find a solution, and those that use ML to guide more traditional heuristic search algorithms. Under the algorithmic framework of solving the MIP, the methods in the later class use ML (including RL), to replace or aid a specific process so that the efficiency of problem solving is improved. [37] tackles the problem of finding an initial feasible solution of a complex MIP by RL, in which CNN and MLP networks are used to encode the constraint matrix for informative state representations, and an efficient policy is designed. Other work [13–17] focuses on learning-aided branch-and-bound, and train an RL policy by imitation learning on data obtained by applying a heuristic strong branching approach. Note, we do not compare to ML4CO methods, as they are tailored to MIP and are not applicable to our problem setting.

Many neural combinatorial optimization methods require large datasets for pre-training, such as Pointer Networks [11] and latent space optimization [38–44]. When a large, expertly obtained, dataset is not known upfront, methods typically resort to RL [33, 10, 45–49] to iteratively learn from the objective function. Combinatorial optimization methods using RL are tailored to their application, such as the TSP [50, 33, 10]. When faced with optimising a TSP problem, one is given a set of nodes

¹<https://www.ecole.ai/2021/ml4co-competition/>

and must select the *permutation* for visiting the nodes that leads to the shortest path. [33] first designed an RL method with Pointer Networks [11] that selects the permutation of nodes to visit based on a factorised policy. Follow up work [10] made progress on improving the architecture with attention, as well as training methods such as greedy rollouts. Although we cannot directly apply these RL methods as our problem is not a permutation problem, we can construct baselines from their core components.

Machine Learning for antibody design Several ML/computational approaches for antibody design [51, 52] have been developed, either using physics-based antibody and antigen structure modelling [53–55] and docking [56, 57], or using ML to learn the non-linear relationship between antibody-antigen binding directly from large sequence/structural datasets [52]. Methods such as [58–61] assume the antigen-antibody is available and predict the affinity directly. Various recent generative models have proposed to generate antibody structure from their amino-acid sequences [62–67]. More recently [68] proposed an iterative refinement process to redesign the CDRH3 sequence of antibodies for improving properties such as the neutralising score. The caveat with these methods is that they require pre-training on large datasets. However, the process of collecting large antibody-antigen binding datasets is identified as a challenging problem due to the high cost of simulation [69–72]. In this work, we focus on the applicability of RL to designing antibodies from scratch, and thus do not compare to methods that require substantial pre-training.

3 Background

We first define the general combinatorial optimization problem and introduce Reinforcement Learning as well as the Q-learning RL algorithm, which serves as the basis for Structured Q-learning.

Definition 1 (Combinatorial optimization) *Given a finite combinatorial set \mathcal{X} , a domain of structures \mathbb{S} consisting of all L -tuples of combinatorial variables $\mathbf{s} \in \mathbb{S} = \mathcal{X}^L$, where $L \in \mathbb{N}$, and an objective function $f : \mathbb{S} \rightarrow \mathbb{R}$, the goal of combinatorial optimization is to find the optimal structure \mathbf{s}^* that maximises f .*

$$\mathbf{s}^* = \arg \max_{\mathbf{s} \in \mathbb{S}} f(\mathbf{s}) = \arg \max_{[\mathbf{x}_i]_{i=0}^{L-1}} f([\mathbf{x}_i]_{i=0}^{L-1}) \quad (1)$$

In the context of antibody design the objective function f is a molecular docking simulator that takes an antibody protein sequence and evaluates its binding energy (affinity) towards a target antigen. Example 1 illustrates the combinatorial structure of the antibody sequence space.

Example 1 *For a set \mathcal{X} of amino acids with $\|\mathcal{X}\| = 20$ and a target protein of size $L = 4$, the individual combinatorial variables are amino acids $x \in \mathcal{X}$, ordered to form a protein structure. Below example \mathbf{s} would constitute a valid structure over the combinatorial variables*

$$\mathbf{s} = [\mathbf{x}_i]_{i=0}^{L-1} = [x_0 = A, x_1 = H, x_2 = D, x_3 = W] = AHDW \quad (2)$$

Definition 2 (Markov Decision Process) *A Markov Decision Process (MDP) is defined as a tuple $\mathcal{M} = \langle \mathcal{O}, \mathcal{A}, \mathcal{P}, r, \gamma_r \rangle$, where \mathcal{O} is a finite observation space; \mathcal{A} is a finite action space; $\gamma_r \in (0, 1)$ is the task discount factor; $\mathcal{P} : \mathcal{O} \times \mathcal{A} \times \mathcal{O} \rightarrow [0, 1]$, i.e., $\mathbf{o}_{t+1} \sim p(\cdot | \mathbf{o}_t, \mathbf{a}_t)$; and $r : \mathcal{O} \times \mathcal{A} \rightarrow [0, +\infty)$ is the task reward. We can define the optimal value function by $V^*(\mathbf{o}) = \max_{\pi} \mathbb{E}_{\mathbf{o}}^{\pi} J_{\text{task}}$, where $\mathbb{E}_{\mathbf{o}}^{\pi}$ is the mean rewards over trajectories from policy π starting at observations \mathbf{o}' . The goal of RL is to find the optimal policy π^* of the MDP:*

$$\pi^* = \max_{\mathbf{a}} Q^*(\mathbf{o}, \mathbf{a}) = \max_{\mathbf{a}} \sum_{\mathbf{y} \in \mathcal{O}} \hat{\mathcal{P}}(\mathbf{y} | \mathbf{o}, \mathbf{a}) [r(\mathbf{o}, \mathbf{a}, \mathbf{y}) + \gamma V^*(\mathbf{y})] \quad (3)$$

We develop a method that builds upon Q-learning [73], one of the most successful methods for finite action spaces. Q-learning works by first collecting *Random Evaluations* of actions in the MDP, and then cycling between i) updating the policy using *Critic Targets*, ii) *Policy Evaluation*, and iii) *Policy Improvement*, where the critic is updated with the following *Critic Targets*, with learning rate α ;

$$Q_{k+1}(\mathbf{o}_t, \mathbf{a}_t) \leftarrow Q_k(\mathbf{o}_t, \mathbf{a}_t) + \alpha(r(\mathbf{o}_t, \mathbf{a}_t) + \gamma \max_{\hat{\mathbf{a}}} Q(\mathbf{o}_{t+1}, \hat{\mathbf{a}}) - Q(\mathbf{o}_t, \mathbf{a}_t)) \quad (4)$$

To develop an RL algorithm for flexible structural generation, we want to allow for both sequential generation (of potentially arbitrary length), as well as allocating variables simultaneously to a fixed-length unallocated sequence. Previous works attempt to define similar padded MDP [50], however we believe our MDP formalism to be the first.

Definition 3 (Variable Allocation Markov Decision Process) A variable allocation Markov Decision Process (VAMP) is defined as a tuple $\mathcal{M}_{CO} = \langle \hat{\mathcal{O}}, \hat{\mathcal{A}}, \hat{\mathcal{P}}, \hat{r}, \gamma_{CO} \rangle$, with observations containing both combinatorial variables and masked variables $\hat{\mathbb{S}} = \hat{\mathcal{X}}^L$, where $\hat{\mathcal{X}} = \mathcal{X} \cup \mathbf{MASK}$, with $\mathbb{S} \subset \hat{\mathbb{S}}$, actions $\hat{\mathcal{A}} = \mathcal{X}$. We define a deterministic transition function given as:

$$\hat{\mathcal{P}}(\mathbf{o}_t = [[\mathbf{a}_i]_{i=0}^t, [\mathbf{MASK}]_{t+1}^T], \mathbf{a}_t, \mathbf{o}_{t+1} = [[\mathbf{a}_i]_{i=0}^{t+1}, [\mathbf{MASK}]_{t+2}^T]) = 1 \quad (5)$$

The set of starting observations ² being $[\mathbf{MASK}]_{i=0}^T$. Lastly, the reward function \hat{r} is defined below, where $[\cdot]$ defines a concatenation operator:

$$\hat{r}(\mathbf{o}_t, \mathbf{a}_t, \mathbf{o}_{t+1}) = \begin{cases} 0 & \text{if } t < L - 1 \\ f([\mathbf{a}_i]_{i=0}^{L-1}) & \text{if } t = L - 1 \end{cases} \quad (6)$$

Example 2 We can now show how the same protein from 2 can be constructed under VAMP.

$$\mathbf{o}_4 = \hat{\mathcal{P}}(\hat{\mathcal{P}}(\hat{\mathcal{P}}(\hat{\mathcal{P}}(\mathbf{o}_0 = [\mathbf{MASK}]_0^3, \mathbf{a}_0 = A), \mathbf{a}_1 = H), \mathbf{a}_2 = D), \mathbf{a}_3 = W) = AHDW \quad (7)$$

Note, VAMP global optima is the same global optima of the underlying function (Theorem 1).

Theorem 1 For combinatorial optimization with discount factor $\gamma_{CO} = 1$ under any objective function f , the optimal policy π^* finds a solution \mathbf{s}^* such that $f(\mathbf{s}^*) = \arg \max_{\mathbf{s} \in \mathbb{S}} f(\mathbf{s})$.

Proof: See Appendix A1. □

4 Structured Q-learning

With the above relevant background, we introduce our proposed algorithm **Structured Q-learning**. SQL is an off-policy RL algorithm for combinatorial optimization that consists of four components that introduce structural priors: *structure critic targets*, *structure policy evaluation*, a *structure exploration operator* ϕ , and *structure policy improvement*, as shown in Algorithm 1 in the Appendix.

Random Structure Evaluations In the first step, we sample random structures \mathbf{s} and evaluate them in the environment to obtain rewards for $f(\mathbf{s})$ for the full structures. The observed pairs $\{\mathbf{s}^{(i)}, f(\mathbf{s}^{(i)})\}$ are saved in a buffer (StructBuffer) and used as initial examples to train SQL’s structure critics.

Structure Critic Targets We train a structure critic on the observed structure-reward pairs obtained from the previous step. For a given sequence \mathbf{s} , the critic’s objective is to learn to predict the expected reward $f(\mathbf{s})$ directly. This step can be achieved similarly to the update for the factorised policy (shown in the Appendix in Equation A2), whereby the same training signal, that is, the true reward observed for the complete structure, is propagated at each step of combinatorial variable prediction:

$$\mathcal{S}([\mathbf{a}_i]_{i=1}^t) \leftarrow \mathcal{S}([\mathbf{a}_i]_{i=1}^t) + \alpha \cdot (f([\mathbf{a}_i]_{i=1}^L) - \mathcal{S}([\mathbf{a}_i]_{i=1}^t)) \quad (8)$$

Structure Policy Evaluation A critic is trained to take structures and predict their objective function values; we can perform policy evaluations in order to determine what the exploitative (greedy) structure $\mathbf{s}^* = \arg \max_{\mathbf{s} \in \mathbb{S}} \mathcal{S}(\mathbf{s})$ should be for the next policy improvement step. For this purpose, we use the critic to generate a new structure used to evaluate the objective function. In general, generation can be done either sequentially or simultaneously.

Sequential Generation constructs the greedy sequence from the trained structure critic one step at a time, at each step choosing the output that maximises the sequence score up to this point:

$$\arg \max_{\mathbf{s} \in \mathbb{S}} \mathcal{S}(\mathbf{s}) = \arg \max_{\mathbf{a}_L \in \mathcal{X}} \mathcal{S}(\dots \arg \max_{\mathbf{a}_2 \in \mathcal{X}} \mathcal{S}([\arg \max_{\mathbf{a}_1 \in \mathcal{X}} \mathcal{S}(\mathbf{a}_1), \mathbf{a}_2]) \dots, \mathbf{a}_L]) \quad (9)$$

Simultaneous Generation, rather than iteratively performing step-wise policy evaluations, formulates the generation procedure to directly produce the highest-value sequence, given the current critic:

$$\arg \max_{\mathbf{s} \in \mathbb{S}} \mathcal{S}(\mathbf{s}) = \arg \max_{\mathbf{a}_1 \in \mathcal{X}, \dots, \mathbf{a}_L \in \mathcal{X}} \mathcal{S}([\mathbf{a}_1, \dots, \mathbf{a}_L]) \quad (10)$$

The choice of using a Transformer [74] network for the Structure Critic allows for straight-forward implementation of either generation method, illustrated in Figure 2: In the sequential case, we train

²If there is context to the optimization problem, we can concentrate it to \mathbf{o}_0 .

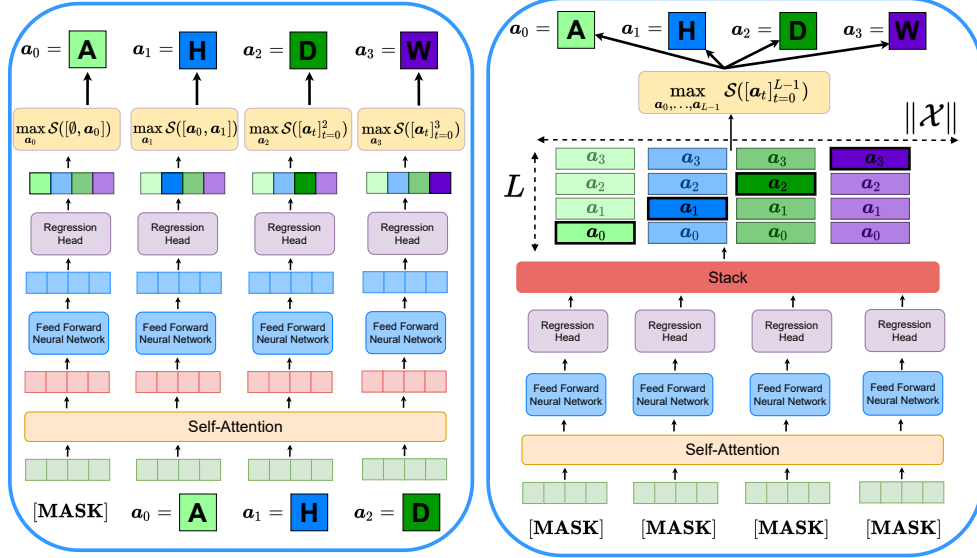


Figure 2: We illustrate two structure policy evaluation strategies implemented with a Transformer. A sequential strategy (Greedy) is shown on the left, and a non-sequential strategy (Masked) shown on the right. Note, both structure policy evaluation strategies take the same input sequence $[MASK]_0^3$ and arrive at the same output sequence $AHDW$ through different computation graphs.

the SQL Critic in a similar fashion to autoregressive Language Models such as GPT[75] with a diagonal attention mask, preventing “lookahead” in the attention mechanism. When aiming for simultaneous generation, the Critic is instead trained similarly to non-autoregressive Masked Language Models like BERT [76] or RoBERTa [77], enabling it to predict multiple variables at the same time.

Structure Exploration Operator $\Phi(\cdot)$ In order to explore new structures during training, we introduce the structure exploration operator $\Phi(\cdot)$. To acquire a random structure for exploration, we uniformly sample a structure $s^{(i)}$ from StructBuffer. We then apply the *replace* operation, which uniformly chooses a substructure x_j and replaces it with another \hat{x} uniformly sampled from $\hat{x} \sim \mathcal{X}$. Note, there are many other available implementations for the operator $\Phi(\cdot)$ e.g. performing crossover between structures, however exploring all operators is out of scope for this work. We define exploitative *structure* as s^* , and random (exploration) structure as \hat{s} .

Structural Policy Improvement Policy improvement trades off when to explore or exploit. We can generalise these exploration strategies to structures. In order to do so, we define a criterion $p(\text{accept} = s^*)$ for selecting either a greedy or a random structure. We propose 3 exploration strategies for $p(\text{accept} = s^*)$, adapted to operate on structures.

e-greedy: An epsilon-greedy (e-greedy) criterion for exploration entails accepting an exploitative action a with probability $p(\text{accept} = a) = 1 - \epsilon_g(n)$, where $\epsilon_g(n) \in [\epsilon_{\min}, 1]$ is a decaying function of steps n . For structures, we use the same criterion for accepting an exploitative *structure* s^* .

S-greedy We introduce a novel criterion based on a secondary structure critic ($S_2(\cdot)$). We do so by comparing the predicted values of S_2 for a random structure \hat{s} and an exploitative structure s^* . If $S_2(s^*) > S_2(\hat{s})$ then $p(\text{accept} = s^*) = 1$, otherwise $p(\text{accept} = s^*) = e^{S_2(\hat{s}) - S_2(s^*)}$.

Sampling: Rather than exploring greedily, we can sample actions from a stochastic policy with probability $p(a | o) = \frac{\exp^{S(o, a)}}{\sum_{a \in \mathcal{X}} \exp^{S(o, a)}}$. This will favour choosing structures with high rewards, but allow for exploration. We fix $p(\text{accept} = s^*) = 1$, as the stochastic policy takes care of exploration.

5 Experiments and Results

First, we introduce antibody design and the molecular docking simulator. Next, we explain our experimental setup and baselines, and lastly, we present the analysis and discussion of the results.

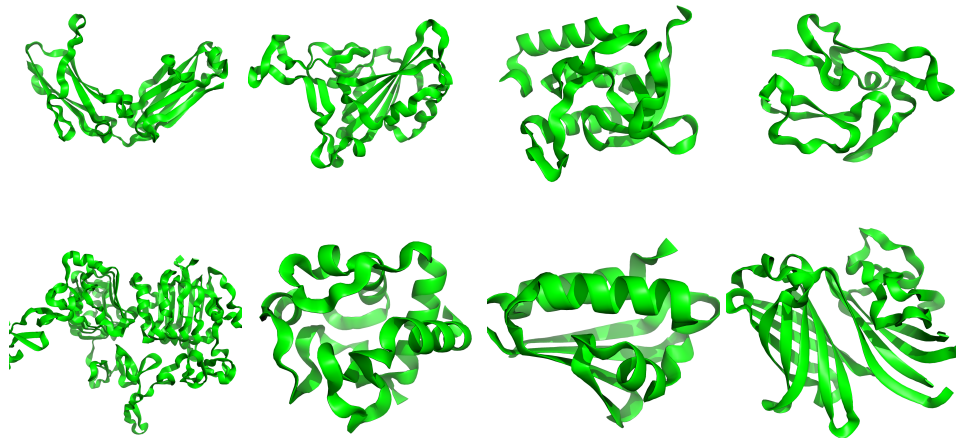


Figure 3: 3D structures of the eight target pathogens selected for antibody tasks. From top left to bottom right; 1ADQ_A, 2DD8_S, 1NSN_S, 1OB1_C, 1S78_B, 1WEJ_F, 2JEL_P, 2YPV_A.

5.1 Experiment Task and Setup

Antibody design problem: Antibodies are large Y-shaped molecules that bind with the antigen at the tip of their variable region [78]. The CDRH3 protein sequence located on the tip of a variable region of the antibody plays a vital role in determining its binding specificity due to its structural diversity [78, 79]. Therefore, one goal of the antibody design process can be finding a protein sequence in the CDRH3 region that would lead to an optimal binding site. An example of a binding site between two proteins is illustrated in the right image in Figure 1. In our work, we use Absolut! [70] to simulate the molecular docking (binding), which computes a lattice view of molecular representation from a sequence and evaluates its binding towards the antigen. We view the Absolut! docking simulator as the objective function, and our goal is to search for a protein sequence, where each character is one of twenty unique Amino Acids ($|\mathcal{X}| = 20$), otherwise referred to as AA’s, that minimizes the binding energy with a target pathogen. Note, the maximum size of input proteins for docking simulation by Absolut! is 11, resulting in an extremely large search space of $|\mathcal{S}| = 2.05 \times 10^{14}$. We demonstrate the applicability of RL methods to solve the above combinatorial optimization problem.

Antibody design tasks: We choose eight highly varied target pathogens to optimise binding energy because of their broad interest in several studies [70, 65]. The eight antigens are IGG4 Fc Region (1ADQ_A), SARS-COV Virus Spike glycoprotein (2DD8_S), SNASE: Staphylococcal nuclease complex (1NSN_S), MSP1: Merozoite Surface Protein 1 (1OB1_C), HER2: Receptor protein-tyrosine kinase erbB-2 (1S78_B), CYC: Cytochrome C (1WEJ_F), ptsH: Phosphocarrier protein HPr (2JEL_P) and fHbp: factor H binding protein (2YPV_A). The first four characters are Protein Data Bank (PDB) followed by a Chain ID. The chain ID identifies a protein responsible for the entering of a pathogen in a host cell. Figure 3 shows the 3D structures of the target pathogens.

SQL and Baseline Settings We evaluate two sequential structured policy evaluation strategies with SQL using beam search with $k=1$ (Greedy) and $k=20$ (Beam). We also evaluate a non-sequential strategy (Masked). For structured policy improvement we use \mathcal{S} -greedy, chosen from experimental results (see ablation results 5.2). We compare to two variations (Critic & MaxB) of a SOTA RL algorithm for combinatorial optimization (with structural priors), adapted to our setting from [33, 10], which we named Structured Policy Gradients (SPG). See Appendix E for details of SPG. Baselines include popular combinatorial optimization algorithm simulated annealing [80] (SA), random search (RS), and the unstructured counterparts of SQL and PG: Q-learning (QL), and policy gradients (PG).

Implementation details In order to ensure we only compare effects from structural priors, all methods use the exact same transformer architecture trained with batch size 32, Adam [81] optimiser with learning rate 0.001. The only differing factor between methods is the manner in which the Transformer is utilised (see Appendix C.1 for exact details of neural architectures). Each trial completed on one Intel Xeon E5 CPU with 200GB RAM.

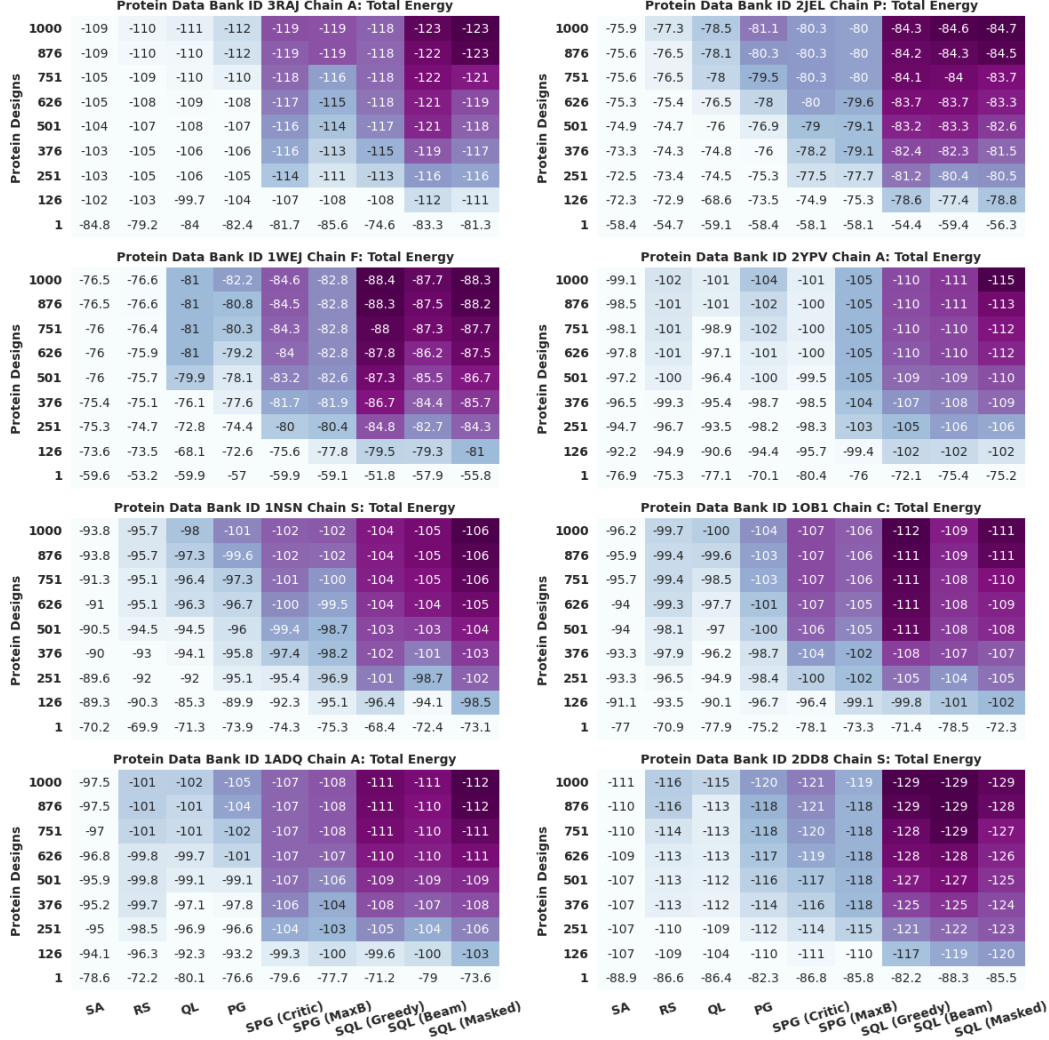


Figure 4: Binding energy performance of baselines and our methods for eight antibody design tasks, averaged across 10 random trials per task. Lower (darker shade) energy is better.

5.2 Results and Discussion

Figure 4 shows heatmap results of the eight antibody design tasks. Each block is a unique antibody design task (see Figure 3). Each column is a method, with each cell being the binding energy averaged over 10 seeds, while the y-axis shows the number of protein designs over time. We colour each cell based on how much it improves upon Simulated Annealing’s final average performance, with darker colours highlighting increased improvement.

We see SQL variants being the top performing amongst off- and on-policy agents. Generally, Q-learning performs worse than policy gradients however, when comparing their combinatorial counterparts (SQL vs SPG), we see this trend reversed. Generally the greedy baseline helps SPG versus using a critic, consistent with [10]. Increasing the beam size from $k=1$ (Greedy) to $k=20$ (Beam) for SQL improves performance slightly however, the highest performing variant is the only non-sequential method evaluated – SQL (Masked). We believe this shows the promise of non-sequential generation of proteins, where the model learns to directly generate the best performing structures.

We are also interested in how different methods perform with respect to a known database of solutions [70]. [65] used quantiles of energy distribution from a known database of 6.9 million (6.9M) biologically obtained proteins to categorise them as low, high, very high, and super binders

Antigens	1ADQ_A	1NSN_S	1OB1_C	1WEJ_F	2YPV_A	3RAJ_A	2JEL_P
Quantiles							
> All 6.9M	-108.53	-107.16	-108.78	-86.03	-114.47	-116.74	-86.05
>0.01%	-102.62	-99.09	-101.56	-79.15	-103.86	-107.95	-79.53
>0.1%	-98.51	-94.85	-97.45	-76.56	-99.92	-104.5	-75.82
>1%	-94.19	-89.99	-92.52	-73.24	-95.18	-100.3	-71.41
>5%	-90.03	-85.46	-88.07	-70.41	-91.16	-96.49	-67.84
>95%	-52.71	-46.64	-46.64	-37.21	-53.62	-53.97	-38.63

Table 1: Energy quantiles of 6.9M experimentally obtained antibody sequences (all sub-sequences of length 11) available from Absolut database [70]. 2DD8_S not reported due to missing data.

Summary: Normalised Total Energy										
Protein Designs	1000	0.799 (-93)	0.834 (-95)	0.857 (-96)	0.903 (-98)	0.932 (-100)	0.936 (-100)	1.002 (-104)	1.007 (-104)	1.031 (-106)
	876	0.796 (-92)	0.829 (-94)	0.848 (-95)	0.886 (-97)	0.929 (-100)	0.935 (-100)	1.0 (-104)	1.003 (-104)	1.024 (-105)
	751	0.775 (-91)	0.825 (-94)	0.838 (-95)	0.865 (-96)	0.927 (-100)	0.923 (-100)	0.996 (-104)	0.997 (-104)	1.009 (-105)
	626	0.767 (-91)	0.814 (-94)	0.824 (-94)	0.842 (-95)	0.919 (-99)	0.915 (-99)	0.989 (-103)	0.989 (-103)	0.997 (-104)
	501	0.761 (-90)	0.803 (-93)	0.807 (-93)	0.824 (-94)	0.905 (-99)	0.902 (-98)	0.978 (-103)	0.976 (-103)	0.98 (-103)
	376	0.746 (-90)	0.789 (-92)	0.778 (-91)	0.804 (-93)	0.881 (-97)	0.885 (-98)	0.954 (-101)	0.951 (-101)	0.958 (-102)
	251	0.736 (-89)	0.769 (-91)	0.754 (-90)	0.785 (-92)	0.851 (-96)	0.865 (-96)	0.919 (-99)	0.909 (-99)	0.928 (-100)
	126	0.714 (-88)	0.74 (-89)	0.662 (-85)	0.738 (-89)	0.781 (-92)	0.815 (-94)	0.841 (-95)	0.844 (-95)	0.869 (-97)
	1	0.438 (-72)	0.361 (-68)	0.449 (-73)	0.409 (-70)	0.455 (-73)	0.437 (-72)	0.333 (-66)	0.439 (-72)	0.392 (-70)
		SA	RS	QL	PG	SPG (Critic)	SPG (MaxB)	SQL (Greedy)	SQL (Beam)	SQL (Masked)

Figure 5: Heat map of normalised (using Table 1) binding energy averaged across antigen tasks and random seeds. We observe SQL (Masked) ranks as the best method and only SQL variants, on average, achieve better energy scores (> 1.0) than all 6.9M biologically obtained proteins.

(top 5/1/0.1/0.01%), based on their binding towards an antigen. This allows for analysing how good the ML methods are in designing sequences over known binding categories. The thresholds of the categories for seven ³ antigens are reported in Table 1. In combination with Figure 4, we can see that SQL reaches high to very high affinity in much fewer evaluations compared to baselines. Moreover, it consistently outperforms the best known sequence available in the database within 1000 evaluations.

Figure 5 further displays the average normalised energy across all random trials and seven antigen tasks ⁴. We normalise using the tail ends (best and worse) of the energy distribution acquired from [70]. A normalised score of > 1.0 means that on average, the method finds antibody sequences with better energy scores than all 6.9M biologically obtained protein sequences. Importantly, *only SQL variants* are able to reach the tremendously difficult average normalized score of ≥ 1.0 . In all cases, we see that structural priors improve performance vs the unstructured equivalent models (QL vs SQL) and (PG vs SPG).

As an example to illustrate the efficacy of SQL for the challenging optimization of antibody designs, Figure 6 shows convergence plots of the tested methods on SARS-COV. We can see that while SQL variants obtain the best energy scores, they do so both fastest and with the lowest standard deviation. This observation can be generalised across all tasks (Appendix Figures A2 and A1).

Analysing the results from all seeds and methods on chain A of 1ADQ, we discovered over 300 unique protein sequences reaching the best binding energy score (-112.59). This highlights the complexity of the problem and how so many related local minima exist. Importantly, $> 99\%$ (all bar three) top performing proteins were found by SQL, showing that SQL is able to consistently find diverse and well performing antibodies when optimising for binding energy over a molecular simulator. See Appendix Figure A3 for additional analysis.

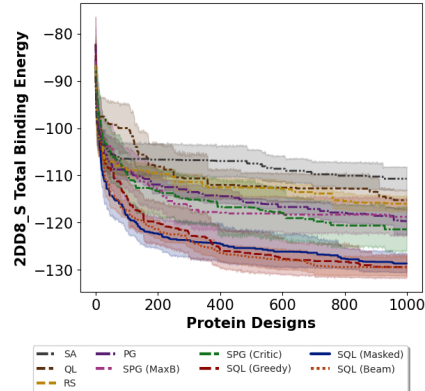


Figure 6: SARS-COV antibody task.

³Not all eight tasks due to missing data for 2DD8_S.

⁴Except 2DD8_S due to the missing quantiles needed for normalisation.

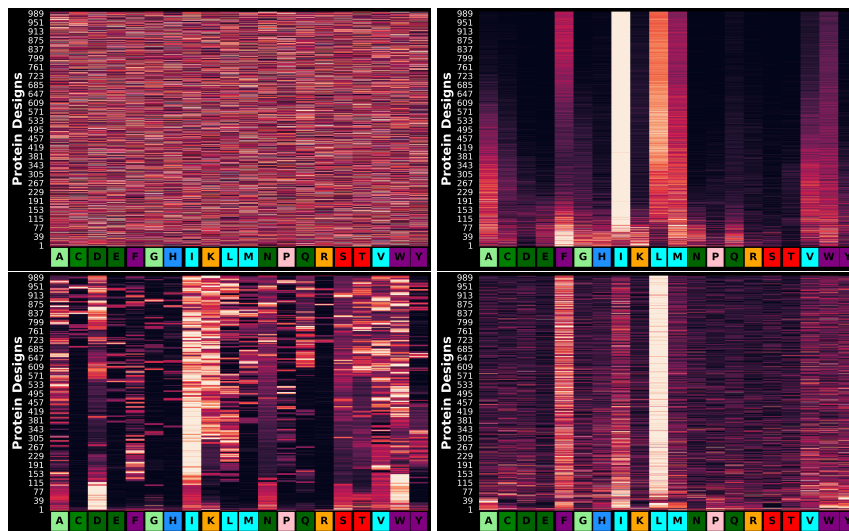


Figure 7: Heatmap of proportions of AA’s selected for SARS-COV (2DD8_S), across 10 seeds per step. The brighter the colour, the higher the proportion. From top left to bottom right: RS, SPG (Critic), QL, SQL. Importantly, we see SQL both focusing on high energy AA’s, as demonstrated in Figure 6, whilst continuing diverse exploration, as shown by bright shading almost everywhere.

This diversity in solutions is further illustrated in Figure 7, which traces the amino acid selection across the optimization process for differing agents on SARS-COV over all seeds. For each amino acid (x-axis), we show the proportion it is selected at each structure suggestion step (y-axis). Both SQL and QL show diverse traces across the task; while QL seems to continue to explore, SQL eventually focuses on exploiting variations of a few core amino acids that provide excellent energy scores. SPG seems to exploit early on, which could explain the under-performance against SQL, which even during the exploitation phase is constantly exploring other solutions.

In the final experiment, we show the influence of varying the policy evaluation and improvement strategies. For each evaluation strategy (greedy, beam search, masked) we run every possible improvement strategy (ϵ -greedy, \mathcal{S} -greedy, sampling⁵). We compare to SPG (Critic), the overall next best performing non-SQL method in previous experiments. We run this ablation study for 20 seeds for each method (Figure 8). It seems the best improvement strategy for all evaluation strategies is \mathcal{S} -greedy, while performance decreases with ϵ -greedy and sampling. Interestingly for masked policy evaluation, sampling seems to quite significantly outperform ϵ -greedy.

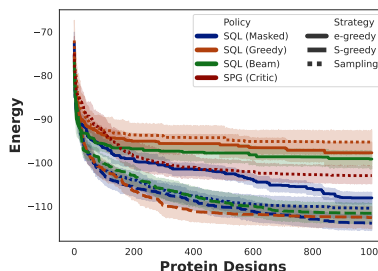


Figure 8: Structural priors ablation.

6 Conclusion and Future Work

We have introduced Structured Q-learning, an extension to classic Q-learning with structural priors. We have demonstrated the effectiveness of SQL on the combinatorial domain of antigen construction. Using a molecular docking simulator we evaluated SQL on optimising protein sequences to bind to various target pathogens, where we observed it significantly improves upon existing RL agents. Importantly, all learning algorithms use the same neural architecture, differing only in how this architecture is utilised. In the future we would like to extend SQL to other combinatorial domains, as well as similarly adapt other off-policy Reinforcement Learning methods for combinatorial optimization.

⁵For Beam we do not include sampling exploration as it can not be implemented together.

References

- [1] Y. Feng, R. Martins, O. Bastani, and I. Dillig, “Program synthesis using conflict-driven learning,” *SIGPLAN Not.*, vol. 53, p. 420–435, jun 2018. (p. 1)
- [2] J. P. M. Silva, I. Lynce, and S. Malik, “Conflict-driven clause learning sat solvers,” in *Handbook of Satisfiability* (A. Biere, M. Heule, H. van Maaren, and T. Walsh, eds.), vol. 185 of *Frontiers in Artificial Intelligence and Applications*, pp. 131–153, IOS Press, 2009. (p. 1)
- [3] L. de Moura and N. Bjørner, “Z3: An efficient smt solver,” in *Tools and Algorithms for the Construction and Analysis of Systems* (C. R. Ramakrishnan and J. Rehof, eds.), (Berlin, Heidelberg), pp. 337–340, Springer Berlin Heidelberg, 2008. (p. 1)
- [4] T. Rocktäschel and S. Riedel, “End-to-end differentiable proving,” in *Advances in Neural Information Processing Systems* (I. Guyon, U. V. Luxburg, S. Bengio, H. Wallach, R. Fergus, S. Vishwanathan, and R. Garnett, eds.), vol. 30, Curran Associates, Inc., 2017.
- [5] P. Minervini, M. Bosnjak, T. Rocktäschel, and S. Riedel, “Towards neural theorem proving at scale,” *CoRR*, vol. abs/1807.08204, 2018. (p. 1)
- [6] R. H. J. M. Otten, “Layout synthesis,” in *Handbook of Algorithms for Physical Design Automation* (C. J. Alpert, D. P. Mehta, and S. S. Sapatnekar, eds.), Auerbach Publications, 2008. (p. 1)
- [7] R. C. Lozano, M. Carlsson, G. H. Blindell, and C. Schulte, “Combinatorial register allocation and instruction scheduling,” *ACM Transactions on Programming Languages and Systems (TOPLAS)*, vol. 41, no. 3, pp. 1–53, 2019. (p. 1)
- [8] A. Grosnit, C. Malherbe, R. Tutunov, X. Wan, J. Wang, and H. Bou-Ammar, “Boils: Bayesian optimisation for logic synthesis,” *CoRR*, vol. abs/2111.06178, 2021. (p. 1)
- [9] I. Bello, H. Pham, Q. V. Le, M. Norouzi, and S. Bengio, “Neural combinatorial optimization with reinforcement learning,” *arXiv preprint arXiv:1611.09940*, 2016. (p. 1)
- [10] W. Kool, H. van Hoof, and M. Welling, “Attention, learn to solve routing problems!,” in *International Conference on Learning Representations*, 2019. (p. 2), (p. 3), (p. 6), (p. 7), (p. 19)
- [11] O. Vinyals, M. Fortunato, and N. Jaitly, “Pointer networks,” *Advances in neural information processing systems*, vol. 28, 2015. (p. 1), (p. 2), (p. 3)
- [12] K. Bestuzheva, M. Besançon, W.-K. Chen, A. Chmiela, T. Donkiewicz, J. van Doornmalen, L. Eifler, O. Gaul, G. Gamrath, A. Gleixner, L. Gottwald, C. Graczyk, K. Halbig, A. Hoen, C. Hojny, R. van der Hulst, T. Koch, M. Lübbecke, S. J. Maher, F. Matter, E. Mühmer, B. Müller, M. E. Pfetsch, D. Rehfeldt, S. Schlein, F. Schlösser, F. Serrano, Y. Shinano, B. Sofranac, M. Turner, S. Vigerske, F. Wegscheider, P. Wellner, D. Weninger, and J. Witzig, “The SCIP Optimization Suite 8.0,” technical report, Optimization Online, December 2021. (p. 1), (p. 2)
- [13] V. Nair, S. Bartunov, F. Gimeno, I. von Glehn, P. Lichocki, I. Lobov, B. O’Donoghue, N. Sonnerat, C. Tjandraatmadja, P. Wang, *et al.*, “Solving mixed integer programs using neural networks,” *arXiv preprint arXiv:2012.13349*, 2020. (p. 2)
- [14] M.-F. Balcan, T. Dick, T. Sandholm, and E. Vitercik, “Learning to branch,” in *ICML*, 2018.
- [15] E. B. Khalil, P. Le Bodic, L. Song, G. L. Nemhauser, and B. N. Dilkina, “Learning to branch in mixed integer programming,” in *AAAI*, 2016.
- [16] M. Gasse, D. Chételat, N. Ferroni, L. Charlin, and A. Lodi, “Exact combinatorial optimization with graph convolutional neural networks,” *arXiv preprint arXiv:1906.01629*, 2019.
- [17] Y. Bengio, A. Lodi, and A. Prouvost, “Machine learning for combinatorial optimization: a methodological tour d’horizon,” *European Journal of Operational Research*, 2020. (p. 1), (p. 2)
- [18] D. Weininger, “Smiles, a chemical language and information system. 1. introduction to methodology and encoding rules,” *J. Chem. Inf. Comput. Sci.*, vol. 28, p. 31–36, feb 1988. (p. 1)

- [19] M. Krenn, F. Häse, A. Nigam, P. Friederich, and A. Aspuru-Guzik, “SELFIES: a robust representation of semantically constrained graphs with an example application in chemistry,” *CoRR*, vol. abs/1905.13741, 2019. (p. 1)
- [20] H. Modjtahedi, S. Ali, and S. Essapen, “Therapeutic application of monoclonal antibodies in cancer: advances and challenges,” *British Medical Bulletin*, vol. 104, pp. 41–59, 10 2012. (p. 1)
- [21] W. H. Organization *et al.*, “mrna vaccines against covid-19: Pfizer-biontech covid-19 vaccine bnt162b2: prepared by the strategic advisory group of experts (sage) on immunization working group on covid-19 vaccines, 22 december 2020,” tech. rep., World Health Organization, 2020. (p. 1)
- [22] D. Cohen, M. Cooper, and P. Jeavons, “A complete characterization of complexity for boolean constraint optimization problems,” in *Proceedings of CP’04*, no. 3258 in Lecture Notes in Computer Science, pp. 212–226, 2004. (p. 1)
- [23] S. A. Cook, “The complexity of theorem proving procedures,” in *Proceedings of the Third Annual ACM Symposium*, (New York), pp. 151–158, ACM, 1971. (p. 1)
- [24] L. De Moura and N. Bjørner, “Satisfiability modulo theories: Introduction and applications,” *Commun. ACM*, vol. 54, p. 69–77, sep 2011. (p. 1)
- [25] E. Ábrahám, J. Abbott, B. Becker, A. M. Bigatti, M. Brain, B. Buchberger, A. Cimatti, J. H. Davenport, M. England, P. Fontaine, *et al.*, “Sc2: Satisfiability checking meets symbolic computation,” *Intelligent Computer Mathematics: Proceedings CICM*, vol. 9791, pp. 28–43, 2016. (p. 2)
- [26] E. Ábrahám, J. H. Davenport, M. England, and G. Kremer, “Deciding the consistency of non-linear real arithmetic constraints with a conflict driven search using cylindrical algebraic coverings,” *CoRR*, vol. abs/2003.05633, 2020.
- [27] G. Kremer, E. Ábrahám, M. England, and J. H. Davenport, “On the implementation of cylindrical algebraic coverings for satisfiability modulo theories solving,” in *2021 23rd International Symposium on Symbolic and Numeric Algorithms for Scientific Computing (SYNASC)*, pp. 37–39, 2021.
- [28] A. I. Cowen-Rivers and M. England, “Summer research report: Towards incremental lazard cylindrical algebraic decomposition,” *ArXiv*, vol. abs/1804.08564, 2018. (p. 2)
- [29] G. E. Collins, “Quantifier elimination for real closed fields by cylindrical algebraic decomposition—preliminary report,” *SIGSAM Bull.*, vol. 8, p. 80–90, aug 1974. (p. 2)
- [30] J. H. Davenport and J. Heintz, “Real quantifier elimination is doubly exponential,” *Journal of Symbolic Computation*, vol. 5, no. 1, pp. 29–35, 1988.
- [31] J. Heintz, “Definability and fast quantifier elimination in algebraically closed fields,” *Theoretical Computer Science*, vol. 24, no. 3, pp. 239–277, 1983. (p. 2)
- [32] A. P. Punnen, *The Traveling Salesman Problem: Applications, Formulations and Variations*, pp. 1–28. Boston, MA, USA: Springer, 2007. (p. 2)
- [33] I. Bello, H. Pham, Q. V. Le, M. Norouzi, and S. Bengio, “Neural combinatorial optimization with reinforcement learning,” *CoRR*, vol. abs/1611.09940, 2016. (p. 2), (p. 3), (p. 6), (p. 19)
- [34] D. Silver, A. Huang, C. J. Maddison, A. Guez, L. Sifre, G. Van Den Driessche, J. Schrittwieser, I. Antonoglou, V. Panneershelvam, M. Lanctot, *et al.*, “Mastering the game of go with deep neural networks and tree search,” *Nature*, vol. 529, no. 7587, pp. 484–489, 2016. (p. 2)
- [35] J. Degraeve, F. Felici, J. Buchli, M. Neunert, B. Tracey, F. Carpanese, T. Ewalds, R. Hafner, A. Abdolmaleki, D. de Las Casas, *et al.*, “Magnetic control of tokamak plasmas through deep reinforcement learning,” *Nature*, vol. 602, no. 7897, pp. 414–419, 2022. (p. 2)

- [36] M. Gasse, Q. Cappart, J. Charfreitag, L. Charlin, D. Chételat, A. Chmiela, J. Dumouchelle, A. Gleixner, A. M. Kazachkov, E. Khalil, P. Lichocki, A. Lodi, M. Lubin, C. J. Maddison, C. Morris, D. J. Papageorgiou, A. Parjadis, S. Pokutta, A. Prouvost, L. Scavuzzo, G. Zarpellon, L. Yang, S. Lai, A. Wang, X. Luo, X. Zhou, H. Huang, S. Shao, Y. Zhu, D. Zhang, T. Quan, Z. Cao, Y. Xu, Z. Huang, S. Zhou, C. Binbin, H. Minggui, H. Hao, Z. Zhiyu, A. Zhiwu, and M. Kun, "The machine learning for combinatorial optimization competition (ml4co): Results and insights," 2022. (p. 2)
- [37] M. Qi, M. Wang, and Z. Shen, "Smart feasibility pump: Reinforcement learning for (mixed) integer programming," *CoRR*, vol. abs/2102.09663, 2021. (p. 2)
- [38] A. Grosnit, R. Tutunov, A. M. Maraval, R. Griffiths, A. I. Cowen-Rivers, L. Yang, L. Zhu, W. Lyu, Z. Chen, J. Wang, J. Peters, and H. Bou-Ammar, "High-dimensional bayesian optimisation with variational autoencoders and deep metric learning," *CoRR*, vol. abs/2106.03609, 2021. (p. 2)
- [39] R.-R. Griffiths and J. M. Hernández-Lobato, "Constrained bayesian optimization for automatic chemical design using variational autoencoders," *Chemical science*, vol. 11, no. 2, pp. 577–586, 2020.
- [40] R. Gómez-Bombarelli, J. N. Wei, D. Duvenaud, J. M. Hernández-Lobato, B. Sánchez-Lengeling, D. Sheberla, J. Aguilera-Iparraguirre, T. D. Hirzel, R. P. Adams, and A. Aspuru-Guzik, "Automatic chemical design using a data-driven continuous representation of molecules," *ACS central science*, vol. 4, no. 2, pp. 268–276, 2018.
- [41] A. Deshwal and J. Dopper, "Combining latent space and structured kernels for bayesian optimization over combinatorial spaces," *Advances in Neural Information Processing Systems*, vol. 34, 2021.
- [42] N. Maus, H. T. Jones, J. S. Moore, M. J. Kusner, J. Bradshaw, and J. R. Gardner, "Local latent space bayesian optimization over structured inputs," *arXiv preprint arXiv:2201.11872*, 2022.
- [43] S. Daulton, D. Eriksson, M. Balandat, and E. Bakshy, "Multi-objective bayesian optimization over high-dimensional search spaces," *arXiv preprint arXiv:2109.10964*, 2021.
- [44] A. Tripp, E. Daxberger, and J. M. Hernández-Lobato, "Sample-efficient optimization in the latent space of deep generative models via weighted retraining," *Advances in Neural Information Processing Systems*, vol. 33, pp. 11259–11272, 2020. (p. 2)
- [45] Q. Ma, S. Ge, D. He, D. Thaker, and I. Drori, "Combinatorial optimization by graph pointer networks and hierarchical reinforcement learning," *arXiv preprint arXiv:1911.04936*, 2019. (p. 2)
- [46] Q. Cappart, D. Chételat, E. Khalil, A. Lodi, C. Morris, and P. Veličković, "Combinatorial optimization and reasoning with graph neural networks," *arXiv preprint arXiv:2102.09544*, 2021.
- [47] M. Boffa, Z. B. Houidi, J. Krolkowski, and D. Rossi, "Neural combinatorial optimization beyond the tsp: Existing architectures under-represent graph structure," *arXiv preprint arXiv:2201.00668*, 2022.
- [48] D. Selsam, M. Lamm, B. Bünz, P. Liang, L. de Moura, and D. L. Dill, "Learning a sat solver from single-bit supervision," *arXiv preprint arXiv:1802.03685*, 2018.
- [49] I. Sutskever, O. Vinyals, and Q. V. Le, "Sequence to sequence learning with neural networks," in *Advances in Neural Information Processing Systems* (Z. Ghahramani, M. Welling, C. Cortes, N. Lawrence, and K. Q. Weinberger, eds.), vol. 27, Curran Associates, Inc., 2014. (p. 2), (p. 19)
- [50] N. Mazyavkina, S. Sviridov, S. Ivanov, and E. Burnaev, "Reinforcement learning for combinatorial optimization: A survey," *Computers & Operations Research*, vol. 134, p. 105400, 2021. (p. 2), (p. 3)

- [51] R. A. Norman, F. Ambrosetti, A. M. Bonvin, L. J. Colwell, S. Kelm, S. Kumar, and K. Krawczyk, "Computational approaches to therapeutic antibody design: Established methods and emerging trends," *Briefings in bioinformatics*, vol. 21, no. 5, pp. 1549–1567, 2020. (p. 3)
- [52] R. Akbar, H. Bashour, P. Rawat, P. A. Robert, E. Smorodina, T.-S. Cotet, F.-K. Karine, R. Frank, B. B. Mehta, M. H. Vu, T. Zengin, J. Gutierrez-Marcos, F. Lund-Johansen, J. T. Andersen, and V. Greiff, "Progress and challenges for the machine learning-based design of fit-for-purpose monoclonal antibodies," *mAbs*, 2022. (p. 3)
- [53] A. Fiser and A. Šali, "Modeller: Generation and refinement of homology-based protein structure models," *Methods in enzymology*, vol. 374, pp. 461–491, 2003. (p. 3)
- [54] J. C. Almagro, A. Teplyakov, J. Luo, R. W. Sweet, S. Kodangattil, F. Hernandez-Guzman, and G. L. Gilliland, "Second antibody modeling assessment (ama-ii)," 2014.
- [55] J. Leem, J. Dunbar, G. Georges, J. Shi, and C. M. Deane, "Abodybuilder: Automated antibody structure prediction with data-driven accuracy estimation," *MAbs*, vol. 8, no. 7, pp. 1259–1268, 2016. (p. 3)
- [56] R. Brenke, D. R. Hall, G.-Y. Chuang, S. R. Comeau, T. Bohnuud, D. Beglov, O. Schueler-Furman, S. Vajda, and D. Kozakov, "Application of asymmetric statistical potentials to antibody-protein docking," *Bioinformatics*, vol. 28, no. 20, pp. 2608–2614, 2012. (p. 3)
- [57] A. Sircar and J. J. Gray, "Snugdock: Paratope structural optimization during antibody-antigen docking compensates for errors in antibody homology models," *PloS computational biology*, vol. 6, no. 1, p. e1000644, 2010. (p. 3)
- [58] V. Morea, A. M. Lesk, and A. Tramontano, "Antibody modeling: Implications for engineering and design," *Methods*, vol. 20, no. 3, pp. 267–279, 2000. (p. 3)
- [59] L. A. Clark, P. A. Boriack-Sjodin, J. Eldredge, C. Fitch, B. Friedman, K. J. Hanf, M. Jarpe, S. F. Liparoto, Y. Li, A. Lugovskoy, *et al.*, "Affinity enhancement of an in vivo matured therapeutic antibody using structure-based computational design," *Protein science*, vol. 15, no. 5, pp. 949–960, 2006.
- [60] L. A. Clark, P. A. Boriack-Sjodin, E. Day, J. Eldredge, C. Fitch, M. Jarpe, S. Miller, Y. Li, K. Simon, and H. W. Van Vlijmen, "An antibody loop replacement design feasibility study and a loop-swapped dimer structure," *Protein Engineering, Design & Selection*, vol. 22, no. 2, pp. 93–101, 2009.
- [61] G. Nimrod, S. Fischman, M. Austin, A. Herman, F. Keyes, O. Leiderman, D. Hargreaves, M. Strajbl, J. Breed, S. Klompus, *et al.*, "Computational design of epitope-specific functional antibodies," *Cell reports*, vol. 25, no. 8, pp. 2121–2131, 2018. (p. 3)
- [62] T. Amimeur, J. M. Shaver, R. R. Ketchum, J. A. Taylor, R. H. Clark, J. Smith, D. Van Citters, C. C. Siska, P. Smidt, M. Sprague, *et al.*, "Designing feature-controlled humanoid antibody discovery libraries using generative adversarial networks," *BioRxiv*, 2020. (p. 3)
- [63] R. R. Eguchi, N. Anand, C. A. Choe, and P.-S. Huang, "Ig-vae: Generative modeling of immunoglobulin proteins by direct 3d coordinate generation," *bioRxiv*, 2020.
- [64] J.-E. Shin, A. J. Riesselman, A. W. Kollasch, C. McMahon, E. Simon, C. Sander, A. Manglik, A. C. Kruse, and D. S. Marks, "Protein design and variant prediction using autoregressive generative models," *Nature communications*, vol. 12, no. 1, pp. 1–11, 2021.
- [65] R. Akbar, P. A. Robert, C. R. Weber, M. Widrich, R. Frank, M. Pavlović, L. Scheffer, M. Chernigovskaya, I. Snapkov, A. Slabodkin, *et al.*, "In silico proof of principle of machine learning-based antibody design at unconstrained scale," *BioRxiv*, 2021. (p. 6), (p. 7)
- [66] R. W. Shuai, J. A. Ruffolo, and J. J. Gray, "Generative language modeling for antibody design," *bioRxiv*, 2021.
- [67] J. Leem, L. S. Mitchell, J. H. Farmery, J. Barton, and J. D. Galson, "Deciphering the language of antibodies using self-supervised learning," *bioRxiv*, 2021. (p. 3)

- [68] W. Jin, J. Wohlwend, R. Barzilay, and T. Jaakkola, “Iterative refinement graph neural network for antibody sequence-structure co-design,” *arXiv preprint arXiv:2110.04624*, 2021. (p. 3)
- [69] P. A. Robert, T. Arulraj, and M. Meyer-Hermann, “Ymir: A 3d structural affinity model for multi-epitope vaccine simulations,” *Iscience*, vol. 24, no. 9, p. 102979, 2021. (p. 3)
- [70] P. A. Robert, R. Akbar, R. Frank, M. Pavlović, M. Widrich, I. Snapkov, M. Chernigovskaya, L. Scheffer, A. Slabodkin, B. B. Mehta, *et al.*, “One billion synthetic 3d-antibody-antigen complexes enable unconstrained machine-learning formalized investigation of antibody specificity prediction,” *BioRxiv*, 2021. (p. 6), (p. 7), (p. 8)
- [71] H. Narayanan, F. Dingfelder, A. Butté, N. Lorenzen, M. Sokolov, and P. Arosio, “Machine learning for biologics: Opportunities for protein engineering, developability, and formulation,” *Trends in pharmacological sciences*, 2021.
- [72] A. H. Laustsen, V. Greiff, A. Karatt-Vellatt, S. Muyldermans, and T. P. Jenkins, “Animal immunization, in vitro display technologies, and machine learning for antibody discovery,” *Trends in Biotechnology*, 2021. (p. 3)
- [73] C. J. Watkins and P. Dayan, “Q-learning,” *Machine learning*, vol. 8, no. 3, pp. 279–292, 1992. (p. 3)
- [74] A. Vaswani, N. Shazeer, N. Parmar, J. Uszkoreit, L. Jones, A. N. Gomez, Ł. Kaiser, and I. Polosukhin, “Attention is all you need,” *Advances in neural information processing systems*, vol. 30, 2017. (p. 4)
- [75] T. Brown, B. Mann, N. Ryder, M. Subbiah, J. D. Kaplan, P. Dhariwal, A. Neelakantan, P. Shyam, G. Sastry, A. Askell, *et al.*, “Language models are few-shot learners,” *Advances in neural information processing systems*, vol. 33, pp. 1877–1901, 2020. (p. 5)
- [76] J. Devlin, M.-W. Chang, K. Lee, and K. Toutanova, “Bert: Pre-training of deep bidirectional transformers for language understanding,” *arXiv preprint arXiv:1810.04805*, 2018. (p. 5)
- [77] Y. Liu, M. Ott, N. Goyal, J. Du, M. Joshi, D. Chen, O. Levy, M. Lewis, L. Zettlemoyer, and V. Stoyanov, “Roberta: A robustly optimized bert pretraining approach,” *arXiv preprint arXiv:1907.11692*, 2019. (p. 5)
- [78] C. Chothia and A. M. Lesk, “Canonical structures for the hypervariable regions of immunoglobulins,” *Journal of Molecular Biology*, vol. 196, pp. 901–917, Aug. 1987. (p. 6)
- [79] J. L. Xu and M. M. Davis, “Diversity in the cdr3 region of vh is sufficient for most antibody specificities,” *Immunity*, vol. 13, no. 1, pp. 37–45, 2000. (p. 6)
- [80] D. Bertsimas and J. Tsitsiklis, “Simulated annealing,” *Statistical science*, vol. 8, no. 1, pp. 10–15, 1993. (p. 6)
- [81] D. P. Kingma and J. Ba, “Adam: A method for stochastic optimization,” *arXiv preprint arXiv:1412.6980*, 2014. (p. 6)
- [82] F. Urbina, F. Lentzos, C. Invernizzi, and S. Ekins, “Dual use of artificial-intelligence-powered drug discovery,” *Nature Machine Intelligence*, vol. 4, no. 3, pp. 189–191, 2022. (p. 16)

Checklist

1. For all authors...
 - (a) Do the main claims made in the abstract and introduction accurately reflect the paper’s contributions and scope? [\[Yes\]](#)
 - (b) Did you describe the limitations of your work? [\[Yes\]](#) We discuss limitation of method and experiments in experimental section.
 - (c) Did you discuss any potential negative societal impacts of your work? [\[Yes\]](#)
 - (d) Have you read the ethics review guidelines and ensured that your paper conforms to them? [\[Yes\]](#)

2. If you are including theoretical results...
 - (a) Did you state the full set of assumptions of all theoretical results? [\[Yes\]](#)
 - (b) Did you include complete proofs of all theoretical results? [\[Yes\]](#)
3. If you ran experiments...
 - (a) Did you include the code, data, and instructions needed to reproduce the main experimental results (either in the supplemental material or as a URL)? [\[Yes\]](#) Code and a script included.
 - (b) Did you specify all the training details (e.g., data splits, hyperparameters, how they were chosen)? [\[Yes\]](#) In experiment section and appendix.
 - (c) Did you report error bars (e.g., with respect to the random seed after running experiments multiple times)? [\[Yes\]](#)
 - (d) Did you include the total amount of compute and the type of resources used (e.g., type of GPUs, internal cluster, or cloud provider)? [\[Yes\]](#)
4. If you are using existing assets (e.g., code, data, models) or curating/releasing new assets...
 - (a) If your work uses existing assets, did you cite the creators? [\[Yes\]](#)
 - (b) Did you mention the license of the assets? [\[N/A\]](#)
 - (c) Did you include any new assets either in the supplemental material or as a URL? [\[Yes\]](#)
 - (d) Did you discuss whether and how consent was obtained from people whose data you're using/curating? [\[N/A\]](#)
 - (e) Did you discuss whether the data you are using/curating contains personally identifiable information or offensive content? [\[N/A\]](#)
5. If you used crowdsourcing or conducted research with human subjects...
 - (a) Did you include the full text of instructions given to participants and screenshots, if applicable? [\[N/A\]](#)
 - (b) Did you describe any potential participant risks, with links to Institutional Review Board (IRB) approvals, if applicable? [\[N/A\]](#)
 - (c) Did you include the estimated hourly wage paid to participants and the total amount spent on participant compensation? [\[N/A\]](#)

Appendices

A Ethical Considerations & Potential Negative Societal Impacts	16
B Additional Experimentation	16
C Additional Algorithmic Details of SQL	16
C.1 Neural Architectures	16
C.2 Variable Size Structure Exploration	19
D Further Details of VAMP	19
E Structured Policy Gradients	19

A Ethical Considerations & Potential Negative Societal Impacts

It is well known that the methods developed for molecular optimization of therapeutic targets, also have the dual use to optimise for toxic targets [82]. Although domain knowledge is still required in chemistry/ toxicology in order to develop harmful molecules, we must continue to raise awareness of the dual use in order to further engage the community in responsible science.

In Appendix B we present additional experiment results. In Appendix C we present the full algorithm for SQL alongside additional details. In Appendix D we present further details of the variable allocation markov decision process (VAMP). Lastly, in Appendix E we will cover the implementation details of the Structured Policy Gradients baselines.

B Additional Experimentation

In Table A2 we report the standard deviation of all 10 seeds at various stages of optimisation for each task. In Figure A1 we show line-plots for each task with 95% confidence intervals.

In Figure A3 we take the top sequences on PDB 1ADQ, Chain A protein optimization task. All but three of 300 sequences found with best energy scores (-112.59) came from SQL, with two sequences from SPG and one from QL. We use multiple sequence alignment on sequences obtained from QL, SPG and SQL.

C Additional Algorithmic Details of SQL

In this section we will give additional details of SQL. In Algorithm 1 we show the high level algorithm for SQL, which follows the same skeleton as Q-learning (also general off policy RL), however at each step is adapted for combinatorial optimization thus instead of outputting individual actions, each step outputs a full structure (e.g. a sequence of actions).

C.1 Neural Architectures

We will now give details of the neural architectures used. We use an embedding with 32 units to embed the amino acid’s in proteins. We additionally use positional encoding on the embeddings. After a transformer is applied we feed this into an MLP in order to predict the logits (for PG/SPG) and targets (For QL and SQL) required for selecting next substructure. For all methods we use one transformer encoder block with embedding size 32, multi-head attention with 8 heads, 64 feed-forward units, layer norm, ReLU activation’s and dropout probability 0.1. All methods therefore have the exact same number of parameters, making for fair algorithmic comparison. Both QL and SQL have an initial random exploration set to 32.

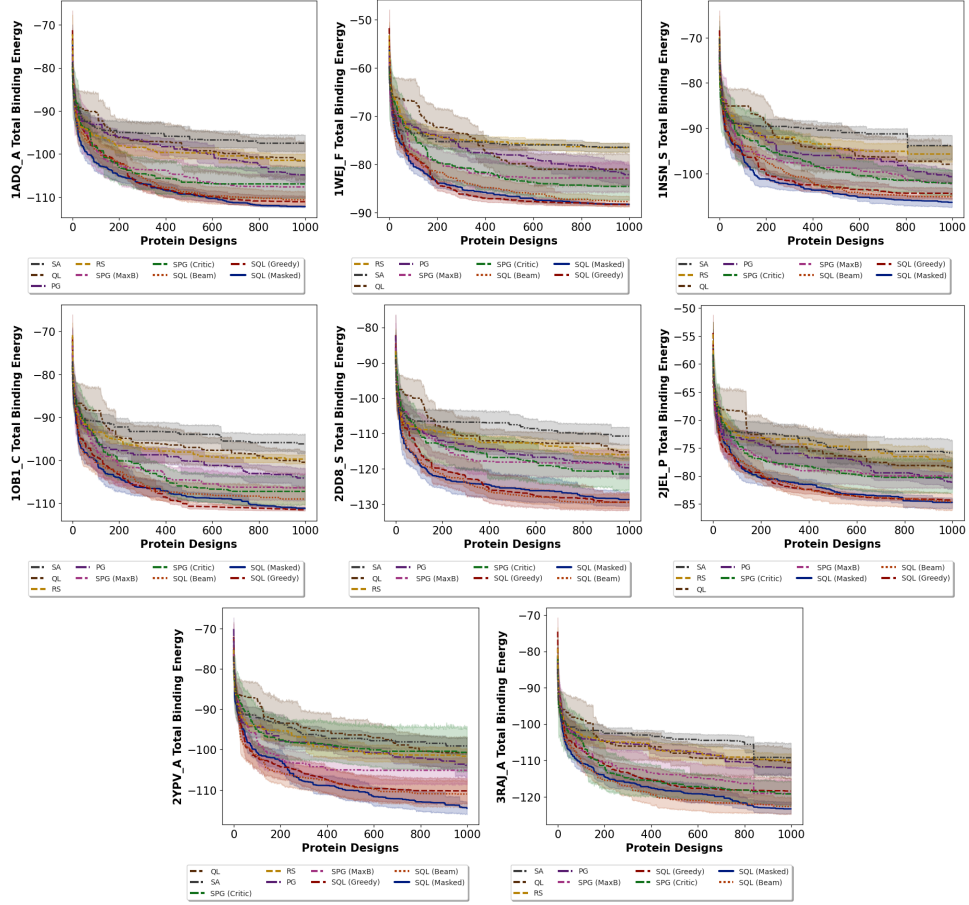


Figure A1: Convergence plots where the x axis indicated number of protein designs evaluated, and the y axis indicates the best energy (lower is better). We observe that across all tasks, SQL variants remain dominant, specifically SQL Masked which generated sequences non-sequentially performs best with the lowest variance.

Algorithm 1: Structured Q-learning

```

Set training steps  $N$ , Set min buffer size  $B$ , StructBuffer  $\leftarrow []$ ;
for  $i$  in range( $N$ ) do
    if  $\text{len}(\text{StructBuffer}) \leq B$  then
        Sample, eval and store  $\{s^{(i)}, f(s^{(i)})\}_{i=0}^B$ 
    else
        Train structure critics e.g.  $\mathcal{S}(\cdot)$ ;
         $s^* = \arg \max_s \mathcal{S}(s)$ ;
        Get rand structure  $\hat{s} \leftarrow \Phi(\text{StructBuffer})$ ;
        if  $p(\text{accept} = s^*)$  then
            Exploit by evaluating structure  $s^*$ , add objective value  $f(s^*)$  to StructBuffer
        else
            Explore by evaluating structure  $\hat{s}$ , add objective value  $f(\hat{s})$  to StructBuffer

```

C.1.1 Variable Size Structures

For variable length sequences, we simply add an additional end of sequence action [EOS] to actions which would stop generation and finalise that this is a complete structure ready for evaluation. For

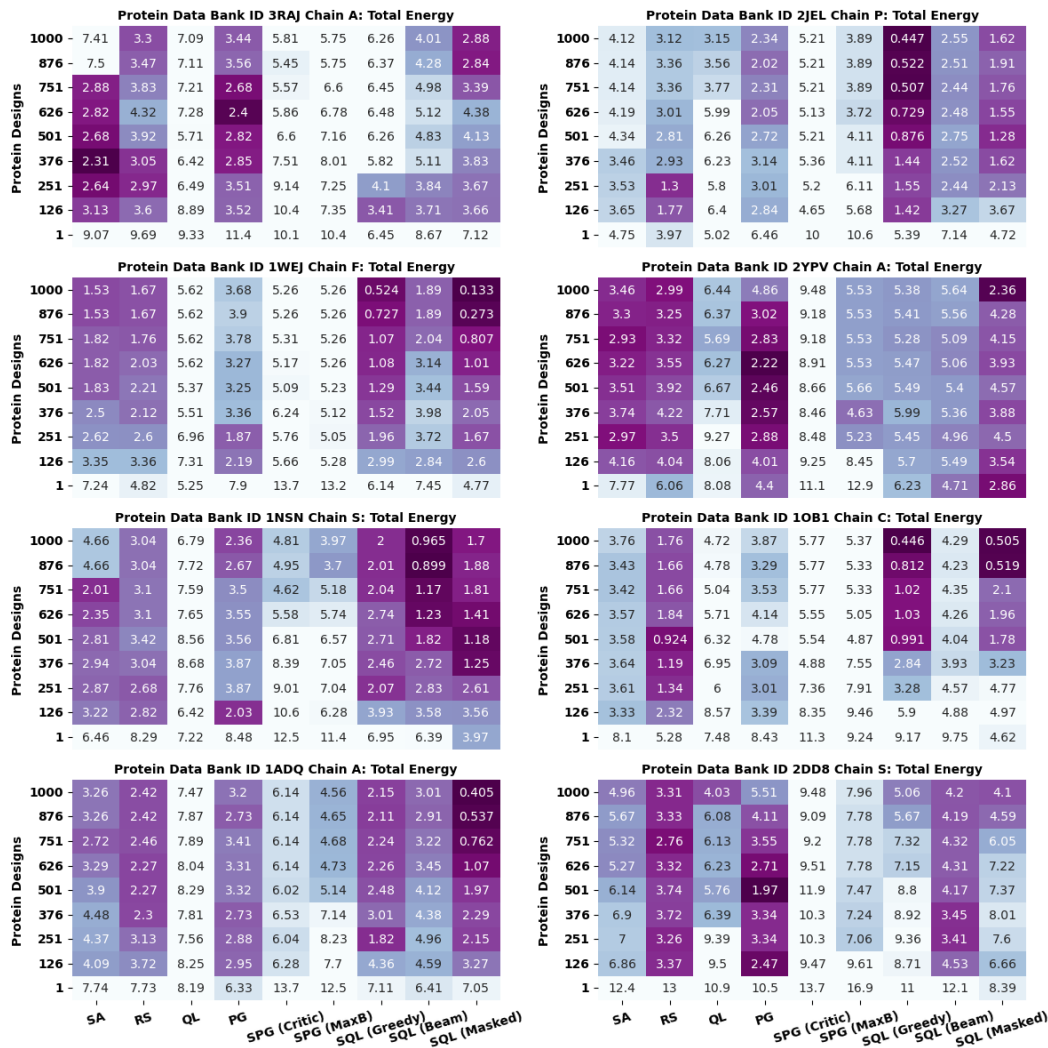


Figure A2: Plot of standard deviations for same intervals as 1



Figure A3: Multiple sequence alignment (MSA) analysis of top proteins found by all agents for the PDB 1ADQ Chain A interaction energy task. The only method that found these energy scoring proteins was SQL variants. Overall for PDB 1ADQ Chain A, SQL variants found over 300 unique proteins with the same objective function value (total energy) of -112.59 . This MSA plot highlights the complexity of the problem and how so many, related, local minima exist.

variable size structures we must also modify the reward function, such that it evaluates the structure in the objective function if the end of structure token **EOS** is present.

C.2 Variable Size Structure Exploration

If one is dealing with variable length structures then we can add two additional operations *shrink* & *expand*, choosing first which operation to apply, then applying the operation to the sampled structure $s^{(i)}$. Where *shrink* deletes a substructure and *expand* adds a uniformly sampled substructure, at a uniformly chosen position in the structure. The other, more standard way to acquire a random structure, would be to just a random uniform set of variables.

D Further Details of VAMP

We will now present the proof of Theorem 1.

Theorem A1 *For $\gamma_{CO} = 1$ and any objective function f , the optimal policy π^* picks a solution s^* such that $f(s^*) = \arg \max_{s \in \mathbb{S}} f(s)$.*

Proof: Using the identity $o_L = [a_i]_{i=0}^{L-1} = [x_i]_{i=0}^{L-1} = s$, we can show

$$\pi^* = \arg \max_{\pi} \mathbb{E} \left[\sum_{t=0}^{L-1} \gamma^t r(o_t, a_t, o_{t+1}) \right] = \arg \max_{\pi} \mathbb{E} [f([a_0, \dots, a_{L-1}])] = \arg \max_{s \in \mathbb{S}} f(s) = s^*$$

□

E Structured Policy Gradients

Structured Policy Gradients (SPG) aim to learn a policy $p(\pi)$ that will assign high probability to combinatorial variables that will improve the objective function, and low probabilities combinatorial variables that will not. As previously formulated in [33, 10, 49], who define Structured Policy Gradients policy using the chain rule to factorize the combinatorial variables:

$$\log p(s) = \log p([a_i]_{i=1}^L) = \sum_{i=1}^L \log p(a_i \mid [a_j]_{j=1}^i) \quad (\text{A1})$$

The authors of [10] identify that for the TSP problem, it can be useful to set a greedy baseline $b(s)$. However, this greedy baseline equates to an additional objective function evaluation per parameter update. For many combinatorial optimization problems the objective function is extremely expensive, hence we are in need of a cheaper baseline. We propose to use the (cheaper) best objective function value observed so far as a greedy policy estimate. For some learning rate α_k at step k , we get the following update for policy parameters θ ;

$$\theta \leftarrow \theta + \alpha_k \cdot \mathbb{E}_{\tau \sim \pi_{\theta}} [\nabla \log p(s) f(s) - b(s)] \quad (\text{A2})$$

In our experiments, we compare SPG with both a learnt baseline (Critic), as done in [33] and greedy baseline (MaxB), as done in [10]